Published in final edited form as:

Nature. 2010 October 14; 467(7317): 854–858. doi:10.1038/nature09446.

Anthrax toxins cooperatively inhibit endocytic recycling by the Rab11/Sec15 exocyst

Annabel Guichard[1], **Shauna M. McGillivray**[2,3,§], **Beatriz-Cruz Moreno**[1,§], **Nina M. van Sorge**[2,§], **Victor Nizet**[2,4], and **Ethan Bier**[1]

[1]Section of Cell and Developmental Biology, University of California, San Diego, 9500 Gilman Drive, La Jolla, CA 92093-0349

[2]Department of Pediatrics, University of California, San Diego, 9500 Gilman Drive, La Jolla, CA 92093-0687

[3]Department of Biology, Texas Christian University, 2800 South University Drive, Fort Worth TX 76129

[4]Skaggs School of Pharmacy & Pharmaceutical Sciences, University of California, San Diego, 9500 Gilman Drive, La Jolla, CA 92093-0687

Abstract

Bacillus anthracis is the causative agent of anthrax in humans and other mammals[1, 2]. In lethal systemic anthrax, proliferating bacilli secrete large quantities of the toxins lethal factor (LF) and edema factor (EF), leading to widespread vascular leakage and shock. While host targets of LF (MAPKKs) and EF (cAMP-dependent processes)[3] have been implicated in the initial phase of anthrax[1, 2], less is understood about toxin action during the final stage of infection. Here, we use *Drosophila* to identify the Rab11/Sec15 exocyst, which acts at the last step of endocytic recycling, as a novel target of both EF and LF. EF reduces levels of apically localized Rab11, and indirectly blocks vesicle formation by its binding partner and effector Sec15 (Sec15-GFP), while LF acts more directly to reduce Sec15-GFP vesicles. Convergent effects of EF and LF on Rab11/Sec15 inhibit expression of and signaling by the Notch ligand Delta and reduce DE-cadherin levels at adherens junctions (AJ). In human endothelial cells, the two toxins act in a conserved fashion to block formation of Sec15 vesicles, inhibit Notch signaling, and reduce cadherin expression at AJ. This coordinated disruption of the Rab11/Sec-15 exocyst by anthrax toxins may contribute to toxin-dependent barrier disruption and vascular dysfunction during *B. anthracis* infection.

Bacillus anthracis (B.a.), the etiologic agent of anthrax, secretes three factors which are required for systemic virulence[1–3]: the toxic enzymatic moieties LF and EF, and protective antigen (PA), which promotes entry of LF and EF into host cells. LF is a zinc

Correspondence to: Ethan Bier.

§These three authors contributed equally to this study

Author contributions: All authors participated in designing the experiments. A.G., and B.C-M. carried out the *Drosophila* experiments. S.M.M. and N.M.V-S carried out the experiments with vertebrate cells and mice. E.B. wrote the manuscript with all other authors providing significant input.

metalloprotease that cleaves and inactivates most human MAPKKs[4, 5], and EF is a potent calmodulin-dependent adenylate cyclase[6]. It has been speculated that additional host targets may contribute to mediating the lethal effects of anthrax toxins[7] and interactions between the two toxins remain poorly understood.

We chose *Drosophila melanogaster* as a model system to identify new candidate pathways involved in anthrax pathogenesis. LF and EF act on conserved signaling components, MAPKKs and PKA, respectively, when expressed directly within cells of transgenic flies, bypassing the need for PA-mediated endocytosis[8]. Here, we report that strong expression of either LF or EF in the larval wing primordium also produces novel unexpected phenotypes. These phenotypes, including wing notching and thickened veins (Supplementary Fig. 1a–c, Supplementary Fig. 2a), are typical of mutants in the Notch signaling pathway and were strongest for EF when using the same GAL4 driver (e.g., Fig. 1b,c and 1h,i). Consistent with these adult phenotypes, high level expression of either toxin greatly reduced expression of the Notch target genes *wg* and *cut* (Supplementary Fig. 1d>i). We also observed potent dosage sensitive genetic interactions between mutations in Notch pathway components and expression of LF (Supplementary Fig. 2b>f) or EF (Supplementary Fig. 2g>n).

An important unresolved issue is whether LF and EF, which are both required individually for the pathogenicity of *B.a.*, also interact in some concerted fashion[9]. We tested for toxin synergy by co-expressing them with a weak ubiquitous wing-specific GAL4 driver. Expression of LF alone produced no obvious phenotype (Fig. 1b; compare to wild-type in 1a). Similarly, expression of only EF resulted in mild occasional notching of the wing margin (Fig. 1c), although it also caused an unrelated phenotype consisting of small wings with altered vein spacing. When EF and LF were co-expressed with this GAL4 driver, however, strong and penetrant wing margin notching phenotypes were superimposed on the EF patterning phenotype (Fig. 1d). Correspondingly, expression of the Notch target gene *wg* (Fig. 1a–d, lower panels) and a Notch reporter construct (not shown) were greatly reduced in LF+EF wing discs. Synergy between LF and EF was also observed using other drivers, such as stgG4 (Fig. 1h–j) and *dpp*G4 (data not shown).

These initial phenotypic observations lead us to examine the mechanisms underlying the Notch inhibitory effects of the anthrax toxins. Both LF (Fig. 1e,f; Supplementary Fig. 3c) and EF (Fig. 1e,g) greatly reduced levels of the Notch ligand Delta (Dl) at the apical surface of wing discs, which we confirmed by selective staining for extracellular Dl expression (Supplementary Fig. 3a–c), and modestly decreased apical levels of Notch (Supplementary Fig. 3g–i). EF also significantly reduced surface expression of a second Notch ligand Serrate (Supplementary Fig. 3d,e). We conclude that both LF and EF inhibit trafficking of the Dl to the apical cell surface, diminishing Notch signaling.

Activation of Dl requires initial cell surface expression followed by endocytosis and recycling (reviewed in[10]), targeting it to the adherens junction (AJ) where it engages the Notch receptor[11]. Small GTPases from the Rab family mediate specific steps of this process[12]. We expressed dominant negative forms of each of the *Drosophila* Rab proteins (RabDN)[13] and identified a single dominant negative factor, Rab11DN, that produced phenotypes virtually identical to those caused by EF (Fig. 1i,k; Supplementary Fig. 4b,c;

Supplementary Table 1). Reciprocally, we co-expressed wild-type forms of each Rab with EF to determine whether increasing their dosage could rescue the Notch-like EF phenotype and found that only Rab11 could suppress EF activity (Fig. 1l,m; compare to 1i; Supplementary Table 1). Consistent with Rab11 mediating the inhibition of Notch signaling by EF, co-expression of Rab11DN with EF greatly enhanced its wing phenotypes (Fig. 1n), and Rab11DN, like EF, could synergize with LF to produce a stronger phenotype (Fig. 1o; similar to 1j). Rab11DN also mimicked the effect of EF in blocking Dl trafficking to the cell surface (Supplementary Fig. 5d–f). A similar role of Rab11 in recycling endocytosed Dl to the apical cell surface has been demonstrated during sensory organ precursor cell development in *Drosophila*[11, 14].

The endogenous Rab11 protein is distributed as small grainy particles just below the apical plasma membrane in wild-type wing discs (Fig. 2a,[11]). In EF-expressing discs, the level of apical Rab11 expression was greatly diminished (Fig. 2b) and ectopic Rab11-positive vesicles appeared in basolateral areas of the cytoplasm (quantified in Supplementary Table 2). This finding suggests that EF acts, at least in part, by reducing the amount and/or altering the distribution of the Rab11 GTPase. Since Rab11 has been implicated in targeting other proteins to the AJ in addition to Notch signaling components[15], we examined expression of several AJ proteins. In wild-type wing discs, the homophylic adhesion molecule DE-cadherin (DECad) is expressed at points of cell-cell contact (Fig. 2d), where it co-localizes with Dl (Supplementary Fig. 5a–c). In contrast, EF precipitously reduced DECad expression at the AJ (Fig. 2e), mimicking the effect of inhibiting Rab11 function (Fig. 2f, Supplementary Fig. 6a,b). This down-regulation of DECad by EF could be partially rescued by co-expression with Rab11wt (Supplementary Fig. 5g–i). Similar, albeit less dramatic, reductions were observed for the AJ proteins α-catenin and β-catenin (Supplementary Fig. 6d,e and g,h respectively), however, Discs Large (Dlg) expression was unaltered (Supplementary Fig. 6j,k) indicating that EF acts selectively and does not lead to gross disruption of AJ integrity *per se*.

As Rab11 interacts with its effector Sec15 to initiate formation of the exocyst complex leading to fusion of the endosome with the plasma membrane (reviewed in[12]), we examined the effect of EF on expression of a *Drosophila* Sec15-GFP fusion protein construct[11]. Sec15-GFP expression has two staining components (Fig. 2g): large round structures near the cell surface, and diffuse cytoplasmic staining. Vesicular Sec15-GFP, which corresponds to a late endocytic compartment poised to fuse with the plasma membrane [11, 16–18], co-localized with Rab11 (Fig. 2j, Supplementary Fig. 7a), consistent with the known interaction of these two proteins in the exocyst complex[11, 15, 19]. Expression of EF virtually abolished large Sec15-GFP vesicles (Fig. 2h), and the few that remained were typically smaller than those in wild-type discs and did not co-label as strongly with Rab11 (Supplementary Fig. 7a,b). In contrast, the uniform cytoplasmic component of Sec15-GFP staining was largely unaltered by EF. EF most likely blocks formation of large Sec15-GFP vesicles indirectly, via its effect on Rab11, since inhibition of Rab11 by Rab11DN (Fig. 2i) or by Rab11-RNAi (data not shown) had the same effect. Furthermore, co-expression of Rab11wt with EF fully rescued punctate Sec15-GFP expression (Fig. 2k; Supplementary Fig. 8a–c).

Since EF and LF interact synergistically in the wing and both toxins reduce access of Dl to the cell surface, we tested whether LF acted at the same recycling step as EF. Although LF did not appreciably alter Rab11 staining (Fig, 2c), like EF, it nearly eliminated large Sec15-GFP vesicles (Fig. 2l) and residual small Sec15-GFP vesicles no longer strongly co-labeled with Rab11 (Supplementary Fig. 7a,c). In contrast to EF, however, the loss of Sec15-GFP staining was only weakly rescued by co-expression with Rab11wt (Supplementary Fig. 8e,f; compare to b,c for EF). LF also reduced levels of DECad at the apical cell surface (Supplementary Fig. 6a–c), although not as strongly as EF. Consistent with Sec15 being a mediator of the LF Notch inhibitory activity, knockdown of endogenous *sec15* function by RNAi caused Notch-like phenotypes in the wing (Supplementary Fig. 9b,d), although over-expression of wild-type *sec15* had no effect (Supplementary Fig. 9a,c). We conclude that LF and EF converge to inhibit two interacting components of the Rab11/Sec15 exocyst, resulting in reduced Notch signaling and weakened AJ.

We next asked whether EF and LF could disrupt function of the well conserved Rab11/Sec15 exocyst, and its downstream effectors Notch and cadherins, in mammalian systems. Established models of endothelial cell function were selected since Notch signaling plays a central role in vascular remodeling (reviewed in [20]), and cadherins are essential for maintaining vascular integrity[21]. We transfected a mammalian Sec15-GFP construct into human brain microvascular endothelial cells (hBMEC) to visualize the exocyst and observed large vesicles (Fig. 3a,d) similar to those in *Drosophila* wing discs (above), yeast[17], and various mammalian cell types[18]. As in *Drosophila*, treatment with either EF toxin (EF+PA) (Fig. 3b,h) or LF toxin (LF+PA) (Fig. 3c) greatly reduced the number and size of the Sec15-GFP vesicles. Moreover, in the case of EF toxin, co-transfection of cells with Rab11-RFP rescued the formation of large Sec15-GFP vesicles (compare Fig. 3h and 3i). Mirroring other systems, Rab11 and Sec15 co-localized, both in untreated (Fig. 3e–g) and in Rab11-RFP rescued EF-treated endothelial cells (Fig. 3i–k). We conclude that the EF and LF toxins function similarly in human and *Drosophila* cells to disrupt formation of the Rab11/Sec15 exocyst.

Looking downstream of the exocyst, we found that treatment with EF toxin disrupted the strong and uninterrupted pan-cadherin (pCad) expression found at points of cell-cell contact in untreated monolayers of hBMEC (compare Fig. 3b,h with 3a,d), in primary human dermal microvascular endothelial cells (hDMEC, Fig. 3m vs. 3l; Supplementary Fig. 11a,b), and in primary human lung microvascular endothelial cells (hMVEC-L, Supplementary Fig. 12a,b). LF toxin had no clear effect on pCad in hBMEC (Fig. 3c), although levels were moderately reduced in hDMEC (Supplementary Fig. 11c), which form more regular borders than hBMEC.

We also examined the effect of anthrax toxins on Notch signaling in mammalian cells. hBMEC were infected with wild-type (WT) *B.a.* Sterne bacteria, which express both EF and LF, or isogenic mutant bacteria lacking EF (ΔEF), LF (ΔLF), or both toxins (ΔLF+EF or ΔpXO1)[22]. Bacterial anthrax toxin production inhibited hBMEC expression of the Notch target genes *Hes1* (Fig. 3n; quantitated in Supplementary Fig. 10a) and *RBPJ* (Supplementary Fig. 10b), with EF exerting the dominant effect. Notch-dependent regulation of *Hes1* in hBMEC was confirmed using the γ-secretase inhibitor DBZ (Fig. 3n). In

addition, EF toxin treatment of hDMEC or hMVEC-L triggered formation of large and misshapen intracellular vesicles of Dll4 (compare Fig. 3m to 3l; Supplementary Fig. 12a vs. 12b) as observed in *Drosophila*.

Since previous studies have described the effect of anthrax toxins on vascular leakage and pulmonary edema [9, 23, 24], we analyzed endothelial barrier integrity using *in vitro* and *in vivo* assays during infection. Exposure to WT *B.a.* increased the permeability of hBMEC transwell monolayers, an effect principally dependent on EF activity (Fig. 3o). Similarly, purified EF toxin induced dose-dependent hBMEC permeability in the same assay (Supplementary Fig. 10c). Next, individual mice were infected subcutaneously in adjacent locations with WT and mutant strains of *B.a.*[22], followed 6 hours later by intravenous injection of Evans Blue dye (Miles assay[25, 26]). WT *B.a.* induced severe vascular effusion at the site of injection (Fig. 3p), and this effect was greatly attenuated in ΔEF mutant bacteria, but only modestly so in ΔLF mutants (Fig. 3p,q). Similarly in the lung, WT *B.a.* induced pulmonary edema, indicative of pulmonary endothelial barrier dysfunction, and this effect too was abrogated in ΔEF mutant bacteria (Supplementary Fig. 12c,d).

In summary, LF and EF toxins interact synergistically in flies to block Rab11/Sec15-dependent endocytic recycling, resulting in reduced Notch signaling and cadherin-dependent adhesion at the AJ, and these toxins produce very similar effects in human cells. Failure to target proteins to the AJ may contribute to the loss of endothelial barrier integrity in EF toxin treated cells and to the toxin-dependent vascular effusion caused *in vivo* during *B.a.* infection (see summary scheme in Fig. 3r). The reduction in Delta/Notch levels in response to anthrax toxin treatment requires further analysis with respect to potential consequences on vascular integrity, which could be direct (e.g., mediated by Notch dependent regulation of factors such as VEGF or by Dl-Notch adhesion) or indirect (e.g., mediated via Notch-dependent regulation of cytokine production). The precise mechanisms by which EF and LF cooperatively inhibit Rab11/Sec15 function remain to be elucidated. EF-mediated cAMP production could act on either or both of two known effectors, protein Kinase A and Epac, both of which have connections to Rab11 regulation[27, 28]. LF may function via cleavage and inactivation of its known MAPKK targets or act on novel targets. Another interesting question is why EF consistently has stronger effects than LF in both flies and vertebrates since they both converge on the exocyst. Perhaps Rab11 has additional partners that act in parallel to Sec15. Alternatively, LF may block only a subset of Sec15 functions or may exert competing effects on the exocyst mediated by opposing actions of different MAPKKs or yet unidentified targets. Future genetic dissection of these impinging pathways will be required to distinguish among these possibilities. It may be fruitful to examine whether the mammalian exocyst and its downstream effectors could also be targets of other microbial virulence factors known to increase cAMP levels, inhibit MAPKK signaling, or disrupt host barrier integrity.

Methods Summary

Drosophila genetics

Transgenic lines UAS-LF2X/FM7, UAS-LF3X/FM7 and UAS-EF UAS-Flp/TM3 were described previously[8]. UAS-Sec15GFP was provided by H. Bellen. UAS-Rab and GAL4

lines were obtained from the Bloomington *Drosophila* stock center. The UAS-*sec15*RNAi stock was obtained from the VDRC.

Immunofluorescence on imaginal discs

Imaginal discs staining involved the following antibodies: Anti-Delta (clone C594.9B-c, Annette Parks), Rat anti-Rab11 (R. Cohen), rat anti-Serrate (K. Irvine). Other antibodies were obtained from the DSHB: anti-Cut (2B10-c), anti-DECAD, anti-α-catenin (D-CAT1), anti β-catenin (N2 7A1) anti-Discs Large (DLG1), and anti-NotchECD (C458 2H). *In situ* hybridization on wing discs was performed as described [29].

hBMEC, hDMEC, and hMVEC-L experiments

hBMEC[30] were infected with *Bacillus anthracis* Sterne ($pXO1^+$, $pXO2^-$) or isogenic mutants[22] and RNA was collected 6 hours later[30] for semi-quantitative PCR and qPCR. For immunofluorescence, hBMEC were transfected using 0.5 μg of DNA (*sec15-GFP*[18] plasmid was kindly provided by C. Mitchell and Rab11-RFP plasmid was a gift from M. Colombo) plus 2 μl Fugene (Roche). Purified EF+PA or LF+PA (S. Leppla) were added for 24 hours and fixed cells were stained using anti-pan-cadherin (Abcam, ab6528) or anti-Dll4 antibodies (Lifespan). For transwell assays, cells were grown on collagenized transwells (Transwell-COL) for 7 days. hDMEC (Lonza CC-2543) or hVMEC-L (Lonza, CC-2527) were treated with purified EF or LF toxin, fixed and stained as described above for hBMEC except that hMVEC-L were treated with EF toxin for 48 hours. Vascular permeability in the skin was assessed using the Miles assay[25, 26].

METHODS

Drosophila genetics

Transgenic lines UAS-LF2X/FM7, UAS-LF3X/FM7 and UAS-EF UAS-Flp/TM3 were described previously[1] UAS-Sec15GFP was kindly provided by Hugo Bellen. UAS-Rab11wt and UAS-Rab11DN, as well as all UAS-Rab transgenic lines, generated by Hugo Bellen, were obtained from the Bloomington *Drosophila* stock center. The UAS-*sec15*RNAi stock is from VDRC (#35161). GAL4 drivers included: stgG4 = MS1096-GAL4, wkG4 =1348-GAL4, ubiG4 = C765-GAL4, L2G4 = E-GAL4, *vg*G4, *dpp*G4 and *brk*G4 have been described previously[2, 3] and are available from the Bloomington *Drosophila* stock or can be obtained upon request.

Immunofluorescence on imaginal discs

Immunostaining of imaginal discs was performed using standard protocols, using the following antibodies: Anti-Delta (clone C594.9B-c was kindly provided by Annette Parks, Boston College and used at 1/1000), anti-*Drosophila* Rab11 antibody (a gift from Robert Cohen, University of Kansas, was used at 1/500), anti-Serrate antibodies (generously provided by Ken Irvine, Waksman Institute for Microbiology, were used at 1/1000). Other antibodies were obtained from the Developmental Studies Hybridoma Bank: anti-Cut (clone 2B10-c, 1/100), anti-DECAD (1/500), anti-αcatenin (D-CAT1, 1/20), anti-βcatenin (Armadillo, clone N2 7A1, 1/20), anti-Discs Large (DLG1, 1/20), and anti-NotchEC (C458 2H, 1/500). *In situ* hybridization on wing discs was performed using a digoxigenin labeled

wg antisense probe as described in Kosman et al. for fluorescent detection[4] or as in O'Neill et al., for histochemical staining[5].

hBMEC, hDMEC, and hMVEC-L experiments

hBMEC[6] were infected with *Bacillus anthracis* Sterne ($pXO1^+$, $pXO2^-$) or isogenic mutants ΔpXO1, ΔLF, ΔEF, or ΔLF/EF[7] and RNA was collected 6 hours later as described previously[6]. Semi-quantitative PCR was performed using 26 cycles and qPCR was performed using iQ SYBR Green supermix (BioRad). For immunofluorescence, hBMEC were treated with indicated amounts of purified EF toxin (Kindly provided by S. Leppla) for 24 hours and stained using mouse anti-pan-cadherin antibody (Abcam, ab6528, 1/100) or anti-Dll4 antibodies (Lifespan) and appropriate secondary antibodies. hBMEC were transfected with *sec15-GFP* plasmid (kindly provided by C. Mitchell, Monash University, Australia) and/or *rab11-RFP* plasmid (a gift from M. Colombo, Universidad Nacional de Cuyo, Argentina) using 0.5 μg of DNA and 2 μl Fugene (Roche). 40 hours after transfection, purified EF+PA or LF+PA were added to the wells and cells were fixed and stained 24 hours later. For transwell assays, cells were seeded on collagenized transwells (Transwell-COL; Corning-Costar Corp., MA, USA) and grown for 7 days at 37°C with 5% CO_2. Cells were infected for 6 hours with bacteria or treated with indicated amounts of EF toxin for 24 hours. 0.4% Evans Blue was added to the upper chamber and leakage was quantified by measuring the color change in the bottom chamber containing HBSS at 620 nm. For DBZ treatment, hBMEC were treated with a final concentration of 2 μM DBZ or vehicle control (DMSO) for 6 hours. For transwell assays, cells were seeded on collagenized transwells (Transwell-COL) and grown for 7 days. Cells were infected for 6 hours with bacteria or treated with indicated amounts of EF toxin for 24 hours. 0.4% Evans Blue was added to the upper chamber and leakage was measured at 620 nm. hDMEC (Lonza CC-2543) or hLMEC (Lonza CC-2527) were treated with purified EF or LF toxin, fixed and stained as described above for hBMEC except that hLMEC were treated with EF toxin for 48 hours.

Vascular permeability assay in mice

Vascular permeability in the skin was assessed using the Miles assay[8, 9]. Nine week old CD-1 female mice were injected with 100 μl PBS containing 1×10^6 CFU *B. anthracis* Sterne, ΔLF and ΔEF bacteria subcutaneously in the hind flank (three spots per mouse). After 6 hours, mice were injected intravenously with 0.1 ml of 2% Evans Blue in PBS and 30 min later mice were euthanized, skins were inverted and examined. For leakage quantification, the site of injection was excised and placed in formamide at 65°C (24 hours) for dye extraction (absorbance 620 nm). Inhibition of Notch signaling in mice was achieved pharmacologically using the γ-secretase inhibitor DBZ. C57Bl/6 female mice were treated for 4 days with 15 μmol/kg of DBZ (n = 5) or vehicle control (n = 8) i.p. On day 5, mice were infected subcutaneously with ΔEF *B.a.* and vascular permeability was assessed using the Miles assay. Statistical significance was assessed using a one-way ANOVA or Student's *t*-test.

Supplementary Material

Refer to Web version on PubMed Central for supplementary material.

Acknowledgments

We thank Adrian Kurciyan for help in analyzing the effects of expressing wild-type and DN forms of Rabs in *Drosophila* and members of the Bier and Nizet labs, Hugo Bellen, and the anonymous reviewers for comments on the manuscript and helpful suggestions. We thank Steven Leppla for providing purified preparations of LF, EF, and PA, and the following investigators for generously providing antibodies: Robert Cohen (anti-Rab11), Annette Parks (anti-Dl), Ken Irvine (anti-Serrate), and Steven Leppla (anti-LF). Support for these studies was provided by NIH R01 grants: AI070654 and NS29870 (E.B.), AI077780 (V.N.), an IRACDA NIH postdoctoral fellowship GM068524 (S.M.M) and a Biomedical Research Fellowship from The Hartwell Foundation (S.M.M).

References

1. Mourez M. Anthrax toxins. Rev Physiol Biochem Pharmacol. 2004; 152:135–64. [PubMed: 15549606]
2. Tournier JN, Quesnel-Hellmann A, Cleret A, Vidal DR. Contribution of toxins to the pathogenesis of inhalational anthrax. Cell Microbiol. 2007
3. Lacy DB, Collier RJ. Structure and function of anthrax toxin. Curr Top Microbiol Immunol. 2002; 271:61–85. [PubMed: 12224524]
4. Duesbery NS, et al. Proteolytic inactivation of MAP-kinase-kinase by anthrax lethal factor. Science. 1998; 280:734–7. [PubMed: 9563949]
5. Vitale G, et al. Anthrax lethal factor cleaves the N-terminus of MAPKKs and induces tyrosine/threonine phosphorylation of MAPKs in cultured macrophages. Biochem Biophys Res Commun. 1998; 248:706–11. [PubMed: 9703991]
6. Leppla SH. Anthrax toxin edema factor: a bacterial adenylate cyclase that increases cyclic AMP concentrations of eukaryotic cells. Proc Natl Acad Sci U S A. 1982; 79:3162–6. [PubMed: 6285339]
7. Moayeri M, Leppla SH. The roles of anthrax toxin in pathogenesis. Curr Opin Microbiol. 2004; 7:19–24. [PubMed: 15036135]
8. Guichard A, Park JM, Cruz-Moreno B, Karin M, Bier E. Anthrax Lethal Factor and Edema Factor act on conserved targets in *Drosophila*. Proc Natl Acad Sci U S A. 2006; 103:3244–9. [PubMed: 16455799]
9. Pezard C, Berche P, Mock M. Contribution of individual toxin components to virulence of Bacillus anthracis. Infect Immun. 1991; 59:3472–7. [PubMed: 1910002]
10. Fortini ME, Bilder D. Endocytic regulation of Notch signaling. Curr Opin Genet Dev. 2009; 19:323–8. [PubMed: 19447603]
11. Jafar-Nejad H, et al. Sec15, a component of the exocyst, promotes notch signaling during the asymmetric division of Drosophila sensory organ precursors. Dev Cell. 2005; 9:351–63. [PubMed: 16137928]
12. Wu H, Rossi G, Brennwald P. The ghost in the machine: small GTPases as spatial regulators of exocytosis. Trends Cell Biol. 2008; 18:397–404. [PubMed: 18706813]
13. Zhang J, et al. Thirty-one flavors of Drosophila rab proteins. Genetics. 2007; 176:1307–22. [PubMed: 17409086]
14. Emery G, et al. Asymmetric Rab 11 endosomes regulate delta recycling and specify cell fate in the Drosophila nervous system. Cell. 2005; 122:763–73. [PubMed: 16137758]
15. Langevin J, et al. Drosophila exocyst components Sec5, Sec6, and Sec15 regulate DE-Cadherin trafficking from recycling endosomes to the plasma membrane. Dev Cell. 2005; 9:365–76. [PubMed: 16224820]
16. Guo W, Roth D, Walch-Solimena C, Novick P. The exocyst is an effector for Sec4p, targeting secretory vesicles to sites of exocytosis. Embo J. 1999; 18:1071–80. [PubMed: 10022848]
17. Salminen A, Novick PJ. The Sec15 protein responds to the function of the GTP binding protein, Sec4, to control vesicular traffic in yeast. J Cell Biol. 1989; 109:1023–36. [PubMed: 2504727]
18. Zhang XM, Ellis S, Sriratana A, Mitchell CA, Rowe T. Sec15 is an effector for the Rab11 GTPase in mammalian cells. J Biol Chem. 2004; 279:43027–34. [PubMed: 15292201]

19. Wu S, Mehta SQ, Pichaud F, Bellen HJ, Quiocho FA. Sec15 interacts with Rab11 via a novel domain and affects Rab11 localization in vivo. Nat Struct Mol Biol. 2005; 12:879–85. [PubMed: 16155582]
20. Roca C, Adams RH. Regulation of vascular morphogenesis by Notch signaling. Genes Dev. 2007; 21:2511–24. [PubMed: 17938237]
21. Dejana E, Tournier-Lasserve E, Weinstein BM. The control of vascular integrity by endothelial cell junctions: molecular basis and pathological implications. Dev Cell. 2009; 16:209–21. [PubMed: 19217423]
22. Janes BK, Stibitz S. Routine markerless gene replacement in Bacillus anthracis. Infect Immun. 2006; 74:1949–53. [PubMed: 16495572]
23. Firoved AM, et al. Bacillus anthracis edema toxin causes extensive tissue lesions and rapid lethality in mice. Am J Pathol. 2005; 167:1309–20. [PubMed: 16251415]
24. Kuo SR, et al. Anthrax toxin-induced shock in rats is associated with pulmonary edema and hemorrhage. Microb Pathog. 2007
25. Gozes Y, Moayeri M, Wiggins JF, Leppla SH. Anthrax lethal toxin induces ketotifen-sensitive intradermal vascular leakage in certain inbred mice. Infect Immun. 2006; 74:1266–72. [PubMed: 16428776]
26. Tessier J, et al. Contributions of histamine, prostanoids, and neurokinins to edema elicited by edema toxin from Bacillus anthracis. Infect Immun. 2007; 75:1895–903. [PubMed: 17261611]
27. Balzac F, et al. E-cadherin endocytosis regulates the activity of Rap1: a traffic light GTPase at the crossroads between cadherin and integrin function. J Cell Sci. 2005; 118:4765–83. [PubMed: 16219685]
28. Silvis MR, et al. Rab11b regulates the apical recycling of the cystic fibrosis transmembrane conductance regulator in polarized intestinal epithelial cells. Mol Biol Cell. 2009; 20:2337–50. [PubMed: 19244346]
29. Kosman D, et al. Multiplex detection of RNA expression in *Drosophila* embryos. Science. 2004; 305:846. [PubMed: 15297669]
30. van Sorge NM, et al. Anthrax toxins inhibit neutrophil signaling pathways in brain endothelium and contribute to the pathogenesis of meningitis. PLoS One. 2008; 3:e2964. [PubMed: 18698416]
1. Guichard A, Park JM, Cruz-Moreno B, Karin M, Bier E. Anthrax Lethal Factor and Edema Factor act on conserved targets in *Drosophila*. Proc Natl Acad Sci U S A. 2006; 103:3244–9. [PubMed: 16455799]
2. Cook O, Biehs B, Bier E. *brinker* and *optomotor-blind* act coordinately to initiate development of the L5 wing vein primordium in *Drosophila*. Development. 2004; 131:2113–24. [PubMed: 15073155]
3. Lunde K, et al. Activation of the *knirps* locus links patterning to morphogenesis of the second wing vein in *Drosophila*. Development. 2003; 130:235–48. [PubMed: 12466192]
4. Kosman D, et al. Multiplex detection of RNA expression in *Drosophila* embryos. Science. 2004; 305:846. [PubMed: 15297669]
5. O'Neill JW, Bier E. Double-label *in situ* hybridization using biotin and digoxigenin-tagged RNA probes. Biotechniques. 1994; 17:870, 874–5. [PubMed: 7840966]
6. van Sorge NM, et al. Anthrax toxins inhibit neutrophil signaling pathways in brain endothelium and contribute to the pathogenesis of meningitis. PLoS One. 2008; 3:e2964. [PubMed: 18698416]
7. Janes BK, Stibitz S. Routine markerless gene replacement in Bacillus anthracis. Infect Immun. 2006; 74:1949–53. [PubMed: 16495572]
8. Gozes Y, Moayeri M, Wiggins JF, Leppla SH. Anthrax lethal toxin induces ketotifen-sensitive intradermal vascular leakage in certain inbred mice. Infect Immun. 2006; 74:1266–72. [PubMed: 16428776]
9. Tessier J, et al. Contributions of histamine, prostanoids, and neurokinins to edema elicited by edema toxin from Bacillus anthracis. Infect Immun. 2007; 75:1895–903. [PubMed: 17261611]

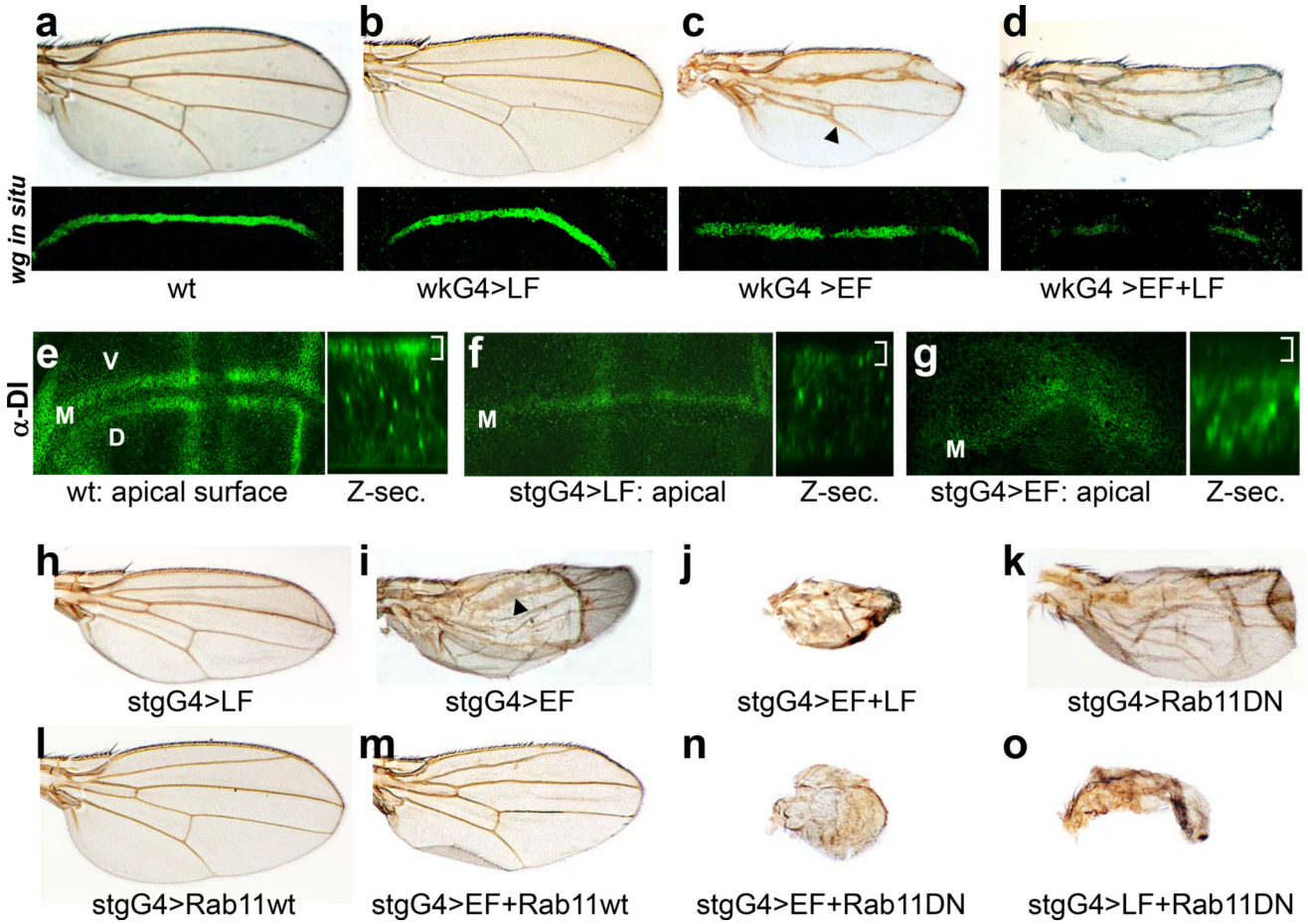

Figure 1. LF and EF synergistically inhibit Notch signaling

a–d) Wings (upper panels) and corresponding wg expression in wing imaginal discs (bottom panels) of the following genotypes: **a**) wild-type (wt), **b**) wkG4>LF2X (wkG4 refers to the 1348-GAL4 driver), **c**) wkG4>EF (wing has A/P patterning phenotype superimposed upon thickened veins - arrowhead - and an occasional small notch at the wing margin), **d**) wkG4>LF2X+EF. **e–g**) Reticular pattern of Delta (Dl) staining in wing discs with accompanying Z-sections. The stgG4 driver is expressed at higher levels on the dorsal - D - surface than on the ventral - V - surface. **e**) Wild-type Dl expression has both cell surface (bracket) and vesicle-like intracellular components, and is expressed along the future margin (M) in two parallel lines as well as in vein primordia (which intersect the margin in perpendicular stripes), **f**) stgG4>LF, **g**) stgG4>EF. **h–o**) wings of the following genotypes: **h**) stgG4>LF, **i**) stgG4>EF (arrowhead indicates thickened veins), **j**) stgG4>LF+EF, **k**) stgG4>Rab11DN, **l**) stgG4>Rab11wt, **m**) stgG4>EF+Rab11wt, **n**) stgG4>EF+Rab11DN, **o**) stgG4>LF+Rab11DN.

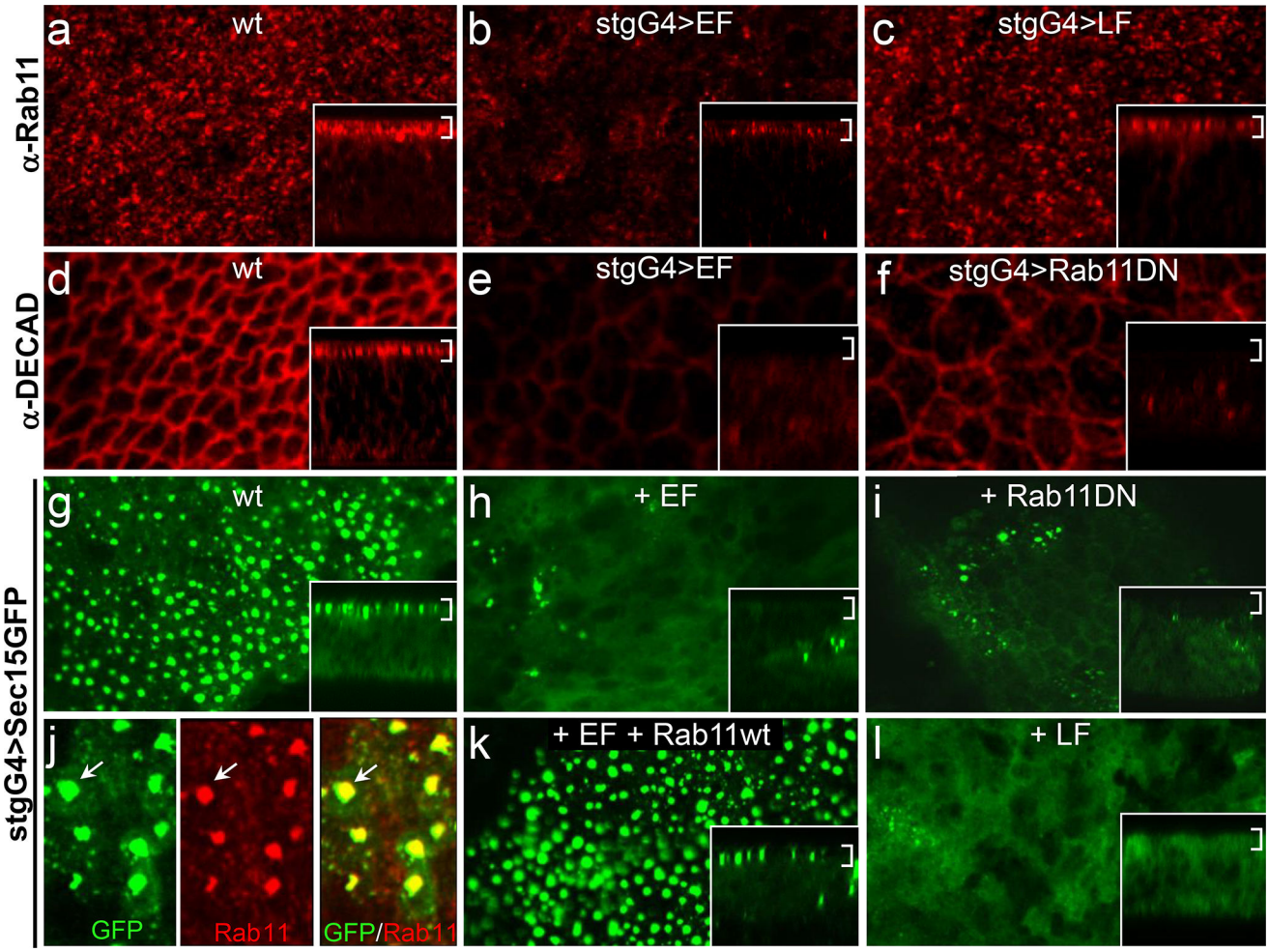

Figure 2. LF and EF inhibit Rab11/Sec15-dependent recycling

a–c) Endogenous Rab11 expression in wing imaginal discs detected by immunofluorescence. Insets are Z-sections from regions of the same discs in these and other panels (brackets indicate the cell surface. **a**) Wild-type, **b**) stgG4>EF, **c**) stgG4>LF disc. **d–f**) DECad expression detected by immunofluorescence. **d**) Wild-type (DECad and Dl co-stain in a net-like pattern at points of cell-cell contact - Supplementary Fig. 4a–c), **e**) stgG4>EF discs, **f**) stgG4>Rab11DN. **g–l**) Expression of a UAS-Sec15-GFP construct driven by the stgG4 driver. **g**) Wild-type - stgG4>Sec15-GFP (large cell surface vesicles of Sec15-GFP co-localize with Rab11 - arrows), **h**) stgG4>EF+Sec15-GFP, **h**) stgG4>Rab11DN+Sec15-GFP (vesicular Sec15-GFP expression is similarly dependent on Rab11=*Sec4* function in yeast[17]), **k**) stgG4>EF+ Rab11wt+Sec15-GFP. **l**) stgG4>LF+Sec15-GFP. Staining differences are quantitated in Supplementary Table 2.

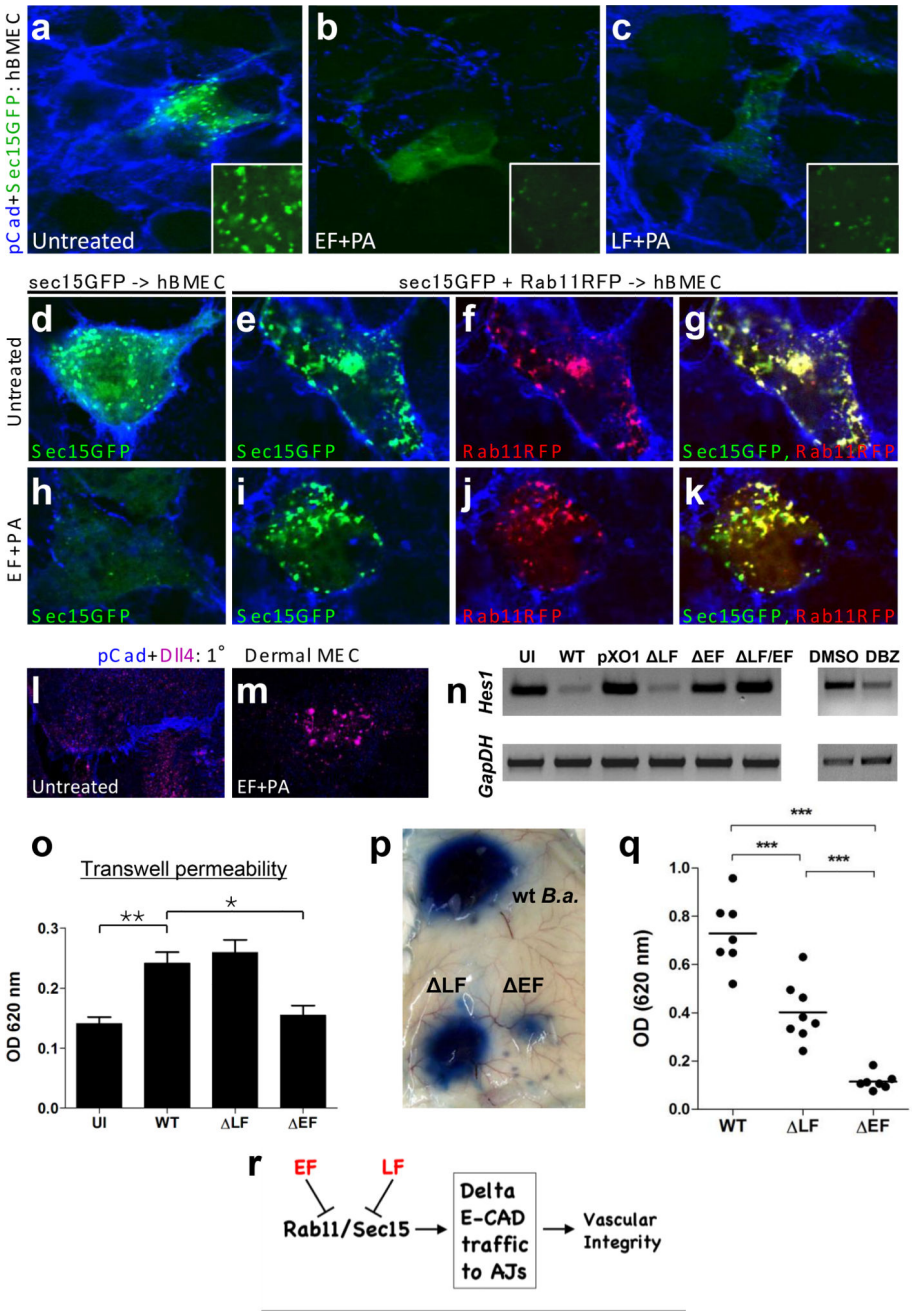

Figure 3. Conserved activity of anthrax toxins in mammals

a–c) Pan-cadherin (pCad) staining (blue) in hBMEC transfected with a human Sec15-GFP construct (green). **a**) Untreated cells. **b**) Cells treated with EF toxin (= 3 μg EF + 6 μg PA) for 24 hours. **c**) Cells treated with LF toxin (= 3 μg LF + 6 μg PA) for 24 hours. Treatment with doses ranging from 0.3 μg to 3 μg gave similar results. **d–k**) Rescue of Sec15-GFP (green) expression by Rab11-RFP (red) in EF toxin treated hBMEC (0.3 μg EF + 0.6 μg PA): **d–g**, untreated cells, and **h–k**, cells treated with 0.3 μg EF + 0.6 μg PA. **d,h**) Cells transfected with Sec15-GFP alone. **e–g, i–k**) cells co-transfected with *sec15*-GFP and wild-type Rab11-RFP. Cells in panels **d–k** were also stained for pCad (blue). **l,m**) Expression of

pCad (blue) and Dll4 (magenta) in untreated primary human dermal microvascular endothelial cells (1° Dermal MEC = hDMEC) (**l**), or after treatment with 1 μg EF + 2 μg PA (**m**). **n**) Semiquantitative analysis of *Hes1* and GapDH RNA expression in hBMEC. First set of lanes: hBMEC infected with *B.a.* or isogenic mutants: UI = uninfected control; WT = *B.a.* Sterne bacteria; ΔpX01 = *B.a.* lacking the pX01 plasmid; ΔLF = *B.a.* with deletion of LF; ΔEF = *B.a.* with deletion of EF; ΔLF/ΔEF = *B.a.* with deletion of both LF and EF. Second set of lanes: effect of the γ-secretase inhibitor DBZ (2 μM) or vehicle control (DMSO) on *Hes1* expression in hBMEC. Staining differences are quantitated in Supplementary Table 2. **o**) Transwell permeability assay of hBMEC cells grown to confluence in a transwell chamber and infected with *B.a.* WT or isogenic toxin mutants. Leakage across the monolayer was determined 6 hours later by measuring Evans Blue leakage to the bottom chamber at OD 620. Abbreviations for genotypes of bacteria are as in panel (**n**). Mean and Standard Deviation (represented by error bars) of a representative experiment are shown. **p**) Vascular effusion in response to subcutaneous infection with *B.a.* (wt *B.a.*) or isogenic toxin mutants ΔLF or ΔEF. Effusion was visualized by Evans blue dye leakage (Supplemental Fig. 9d). **q**) Quantitation of vascular permeability shown in Fig. 3p. ***, $p < 0.001$. **r**) Proposed schematic model for the convergent activity of EF and LF on the exocyst. EF reduces Rab11 levels/activity, which indirectly inhibits formation of Sec15 exocyst complexes, while LF acts more directly on Sec15. The combined effect of these two toxins is to reduce cell surface expression of the Notch ligand Dl and cadherins at AJs, and possibly other AJ proteins involved in cell-cell adhesion and barrier maintenance, thereby compromising vascular integrity.